iScience

CellPress
OPEN ACCESS

Article

High RIPK3 expression is associated with a higher risk of early kidney transplant failure

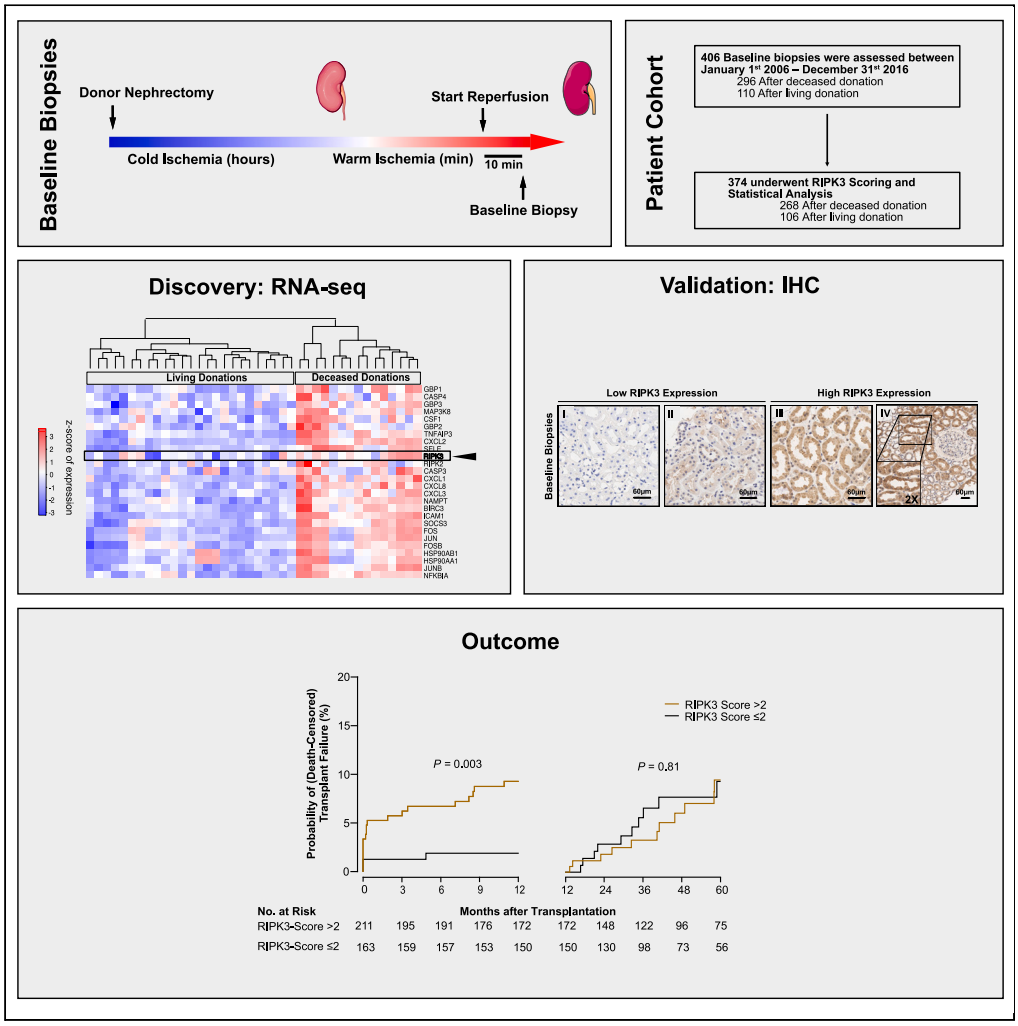

Adam Wahida, Christoph Schmaderer, Maike Büttner-Herold, ..., Jan Hinrich Bräsen, Uwe Heemann, Stephan Kemmner

stephan.kemmner@tum.de

Highlights

First-in-human study comparing RIPK3 expression in renal biopsies with clinical outcome

RIPK3 expression correlates with cold ischemia time

RIPK3 expression is associated with a higher risk of 1-year transplant failure

RIPK3 expression predicts 1-year graft failure independent of recipient risk factors

Wahida et al., iScience 26, 107879
October 20, 2023
https://doi.org/10.1016/j.isci.2023.107879

iScience

CellPress
OPEN ACCESS

Article

High RIPK3 expression is associated with a higher risk of early kidney transplant failure

Adam Wahida,[1,20] Christoph Schmaderer,[2,20] Maike Büttner-Herold,[3] Caterina Branca,[1] Sainitin Donakonda,[4] Flora Haberfellner,[2] Carlos Torrez,[2] Jessica Schmitz,[4] Tobias Schulze,[1] Tobias Seibt,[5] Rupert Öllinger,[6] Thomas Engleitner,[6] Bernhard Haller,[7] Katja Steiger,[8] Roman Günthner,[2] Georg Lorenz,[2] Monica Yabal,[4] Quirin Bachmann,[2] Matthias C. Braunisch,[2] Philipp Moog,[2] Edouard Matevossian,[10] Volker Aßfalg,[11] Stefan Thorban,[9] Lutz Renders,[2] Martin R. Späth,[12,13] Roman-Ulrich Müller,[12,13] Dirk L. Stippel,[14] Wilko Weichert,[8] Julia Slotta-Huspenina,[8] Sibylle von Vietinghoff,[15] Ondrej Viklicky,[16] Douglas R. Green,[17] Roland Rad,[4] Kerstin Amann,[3] Andreas Linkermann,[18,19] Jan Hinrich Bräsen,[4] Uwe Heemann,[2] and Stephan Kemmner[2,5,21,*]

SUMMARY

Renal ischemia-reperfusion injury (IRI) is associated with reduced allograft survival, and each additional hour of cold ischemia time increases the risk of graft failure and mortality following renal transplantation. Receptor-interacting protein kinase 3 (RIPK3) is a key effector of necroptosis, a regulated form of cell death. Here, we evaluate the first-in-human RIPK3 expression dataset following IRI in kidney transplantation. The primary analysis included 374 baseline biopsy samples obtained from renal allografts 10 minutes after onset of reperfusion. RIPK3 was primarily detected in proximal tubular cells and distal tubular cells, both of which are affected by IRI. Time-to-event analysis revealed that high RIPK3 expression is associated with a significantly higher risk of one-year transplant failure and prognostic for one-year (death-censored) transplant failure independent of donor and recipient associated risk factors in multivariable analyses. The RIPK3 score also correlated with deceased donation, cold ischemia time and the extent of tubular injury.

INTRODUCTION

We face a worldwide shortage of organs suitable for kidney transplantation and the demand clearly exceeds the allocable organ numbers.[1] A strategy to increase the pool of donated organs is using kidneys from expanded criteria donors with expected lower quality.[2,3] Thus, organ quality affects early transplant outcome, especially one-year transplant failures.[4] One critical contributor to an early transplant outcome is the extent of renal ischemia-reperfusion injury (IRI) which histologically presents as acute tubular injury.[5–7] Identifying human-relevant cell death pathways during renal IRI could help pinpoint targets to improve organ preservation and safely expand organ supply.[8]

[1]Medical Department III of Hematology and Oncology, Klinikum rechts der Isar, TUM School of Medicine, Technical University of Munich, Munich, Germany
[2]Department of Nephrology, Klinikum rechts der Isar, TUM School of Medicine, Technical University of Munich, Munich, Germany
[3]Department of Nephropathology, Friedrich-Alexander University (FAU) Erlangen-Nurnberg, Erlangen, Germany
[4]Nephropathology Unit, Institute of Pathology, Hannover Medical School, Hannover, Germany
[5]Transplant Center, University Hospital Munich, Ludwig-Maximilians-University (LMU), Munich, Germany
[6]Institute of Molecular Oncology and Functional Genomics, TUM School of Medicine, Technical University of Munich, Munich, Germany
[7]Institute of AI and Informatics in Medicine, Klinikum rechts der Isar, Technical University of Munich, Munich, Germany
[8]Institute of Pathology, TUM School of Medicine, Technical University of Munich, Munich, Germany
[9]Institute of Molecular Immunology and Experimental Oncology, TUM School of Medicine, Technical University of Munich, Munich, Germany
[10]Clinic of General, Visceral, Transplantation, Vascular and Thoracic Surgery, University Hospital Munich, Ludwig-Maximilians-University (LMU), Munich, Germany
[11]Department of Surgery, Klinikum rechts der Isar, Technical University of Munich, Munich, Germany
[12]Department II of Internal Medicine and Center for Molecular Medicine Cologne, University of Cologne, Faculty of Medicine and University Hospital Cologne, Cologne, Germany
[13]CECAD, University of Cologne, Faculty of Medicine and University Hospital Cologne, Cologne, Germany
[14]Department of General, Visceral and Cancer Surgery, University of Cologne, Cologne, Germany
[15]Nephrology Section, Medical Clinic 1, University Hospital Bonn, Rheinische Friedrich Wilhelm University of Bonn, Bonn, Germany
[16]Department of Nephrology, Transplant Center, Institute for Clinical and Experimental Medicine, Prague, Czech Republic
[17]Department of Immunology, St. Jude Children's Research Hospital, Memphis, TN, USA
[18]Division of Nephrology, Clinic of Internal Medicine 3, University Hospital Carl Gustav Carus at the Technische Universität Dresden, Dresden, Germany
[19]Division of Nephrology, Department of Medicine, Albert Einstein College of Medicine, Bronx, NY, USA
[20]These authors contributed equally
[21]Lead contact
*Correspondence: stephan.kemmner@tum.de
https://doi.org/10.1016/j.isci.2023.107879

Several preclinical studies have correlated renal IRI with the activation of a highly inflammatory form of regulated cell death, i.e., necroptosis.[9] The pathway-defining executioner kinase of necroptosis is the receptor-interacting protein kinase 3 (RIPK3).[10] RIPK3-dependent signaling can be triggered by engaging various cell-surface receptors, such as toll-like receptors, tumor-necrosis factors (TNFs), or other death receptors. After engagement, RIPK3 becomes part of an activating protein-multimer capable of eliciting downstream signaling events leading to cell death by releasing damage-associated molecule patterns (DAMPs) and subsequent inflammation.[11–13] Preclinical studies have shown that genetic loss of RIPK3 protects against IRI,[14] particularly in the kidney.[15] Following murine kidney transplantation, recipients of RIPK3 deficient donor kidneys showed improved graft survival compared to controls.[16] Despite these encouraging preclinical data, there is a lack of clinical evidence for the relevance of necroptosis in human pathology such as acute kidney injury and transplantation.[17,18]

To identify relevant markers of regulated cell death pathways in human pathology, we analyzed a large cohort of post-reperfusion baseline biopsies immediately after kidney transplantation. We identified RIPK3 as a possible actionable target in renal IRI and we showed an association between high RIPK3 expression and early kidney transplant outcome.

RESULTS

Transcriptomic analysis of baseline biopsies from living and deceased donors

Transplants from living donors have an improved outcome than deceased donors due to short CIT and the generally robust health condition and renal status of living donors, which are carefully checked before transplantation.[19] To understand the molecular differences behind the better quality of living donor grafts, we performed RNA-sequencing expression profiling on 18 baseline biopsies obtained from living- and deceased-donor grafts (Figure 1A). Principal component analysis confirmed a clear distinction between living and deceased donors (Figure 1B). We identified many differentially expressed genes (DEGs) across groups (up = 478, down = 376, fold change: 1.5, $q < 0.05$) (Table S1). To dissect DEGs' gene-gene interactions, we performed a Weighted Gene Co-expression Network Analysis (WGCNA), which organizes the DEGs into different modules, depending on their transcriptional expression pattern. This analysis yielded five co-expression modules (Figure 1C) and to test each module's expression pattern, we computed the weighted expression profiles (''eigengene'') of each module, which revealed that modules 1, 2, and 5 were significantly upregulated in deceased donors compared to living donors (Figure 1D). In contrast, modules 3 and 4 were downregulated (Figure 1D). Of note, module-wise pathway enrichment analysis identified the TNF signaling pathway as most significantly enriched in module 1 (Figures 1E, 1F, and S1). We further confirmed that TNF signaling was the most significantly upregulated pathway by gene set enrichment analysis (GSEA, Figure 1F, NES: 2.97, FDR <0.0001). We thus focused on this pathway and extracted individual gene expression values to determine which members of this pathway were differentially expressed in both groups (Figure 1G).

TNF signaling as a central hub mediating inflammation can trigger many cellular outcomes.[20] Next to beneficial signaling cues such as NF-κB activation, which can promote regeneration and proliferation, TNF signaling can also be skewed toward different cell death modalities in particular apoptosis and necroptosis. Necroptosis, which per definition is triggered by RIPK3,[10] has been heralded as one of the main contributors to IRI, at least in mice.[16] Nevertheless, we found that most genes that were significantly deregulated could be attributed to an NF-κB-mediated inflammatory response, most likely not implicated in cell death.[12] Furthermore, from all genes implicated in the cell death response downstream of TNF, solely *RIPK3* was upregulated in deceased-versus living-donor grafts (Figure 1H), prompting us to further investigate the importance of RIPK3 in human kidney transplants. Importantly, RIPK3 is a downstream trigger of several TNFR superfamily members, such as TRAIL, TNRF1, Fas receptor (CD95L), and others. The TWEAK receptor FN14 regulates that system. In particular, Bossaller et al.[21] demonstrated that the effects of CD95 on pro-inflammatory RIPK3 activation go beyond classical necroptosis and can involve the maturation of IL-1b and IL-18, the pyroptosis-associated cytokines. RIPK3, therefore, serves as a signaling hub. Very recent data have indicated even non-necroptotic functions of RIPK3, such as the ones demonstrated in mice[22] and previously in cell culture by the group of Degterev.[23] On a separate but equally important consideration, TNF mediates strong pro-survival effects, such as the NF-kB-dependent expression of cFLIP, an anti-apoptosis and anti-necroptotic non-catalytical homolog of caspase-8.[24] The effect was even demonstrated for the human caspase-10.[25] In conclusion, the inhibition or monitoring of TNF or the TNFR1/2 signaling system will most likely not come close to leveling with RIPK3 kinase inhibition. Moreover, this approach might impede the beneficial effects of TNF in the context of renal IRI, such as promoting the regeneration of damaged parenchyma.

Patients

To validate our transcriptomic findings, we examined RIPK3 protein expression in a large cohort of human baseline biopsies by semi-quantitative scoring via immunohistochemistry. A total of 406 post-reperfusion baseline kidney biopsies were performed during surgery between 01.01.2006 and 31.12.2016 at the Klinikum rechts der Isar, Munich. Of these, 385 specimens from 381 patients were available for retrospective analysis (Figure 2A). Four patients were transplanted twice during the observation period due to early transplant failure at first transplantation (two patients due to primary non-function, one patient due to a perioperative complication in the first transplantation, and one patient due to transplant failure within three months). In 21 biopsies, either no biopsy sample was available (18 specimens) or no renal cortex was detectable in the biopsy (three specimens). A total of 24 biopsied renal allograft recipients received an organ that never functioned adequately. Of these, eleven renal allograft recipients had a perioperative complication and had to be excluded from further statistical analysis. Further 13 recipients had a primary non-function (permanent loss of allograft function without perioperative complications) and were considered as transplant failure within first year in the statistical analysis. In conclusion, 374 allografts underwent RIPK3 scoring and were included in the final statistical analysis. All reported data refer to these 374 allografts in 371 different recipients (Table 1). The median follow-up time for recipients at the time of data extraction from the clinical follow-up database (data lock: June 30, 2017) was 4.6 years.

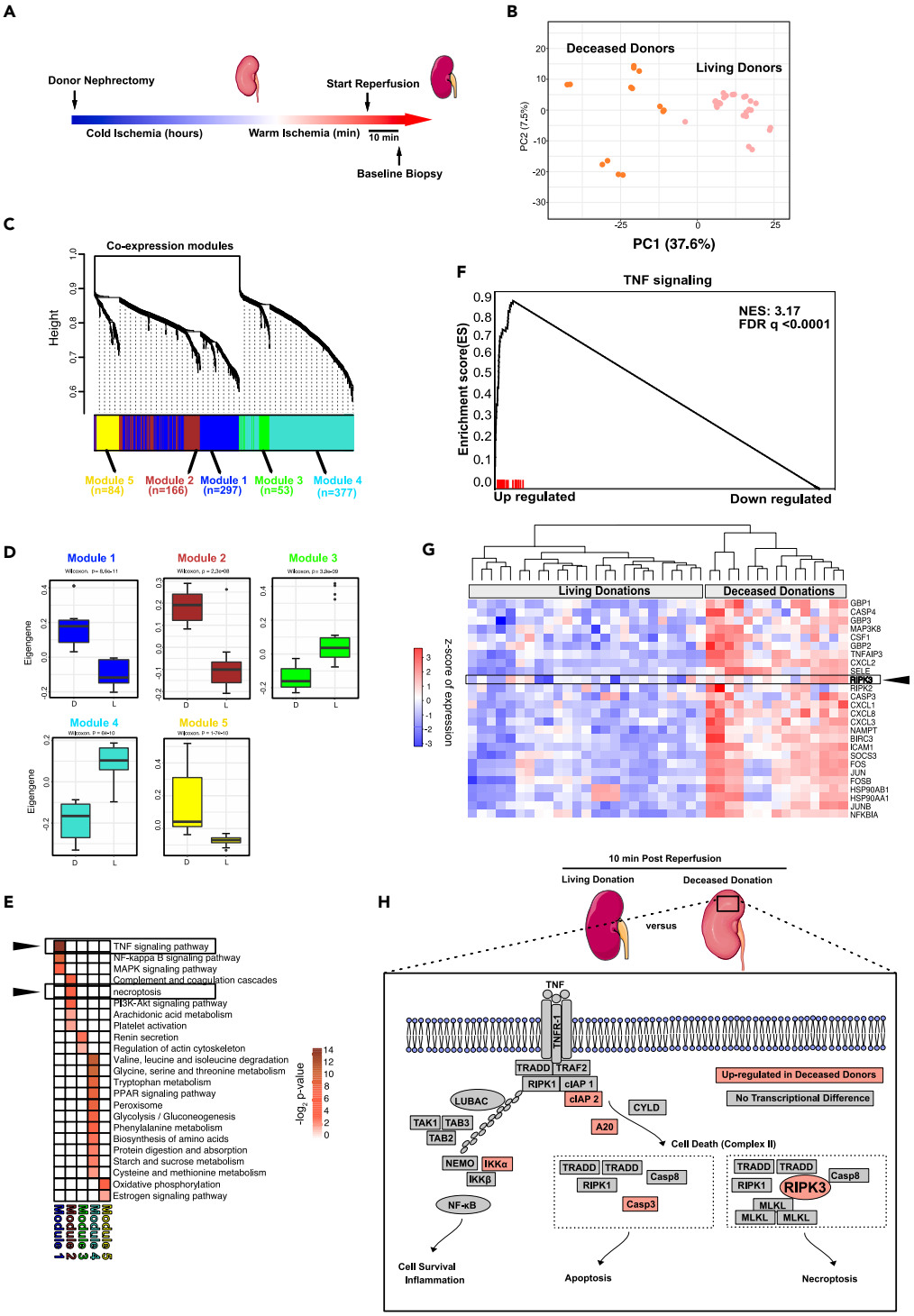

Figure 1. Gene expression analysis of baseline biopsies of deceased versus living donors

(A–D) Schematic workflow showing how baseline biopsies were sampled 10 min after reperfusion of the donor graft (B) Principal component analysis (PCA) between the living and deceased donors' gene expression profiles (C) The dendrogram denotes network modular organization of differentially expressed genes comparing the deceased with living donor dataset (D) Module expression profiles of long ischemia based on the module eigengene.

(E–H) Heatmap represents the KEGG pathway enrichment analysis of each co-expression module as calculated by WGCNA (F) GSEA of the TNF signaling pathway in long ischemia NES, normalized enrichment score (G) Heatmap representing the members of the TNF signaling pathway genes significantly expressed in deceased donors (H) Schematic overview of TNF signaling with members being denoted in magenta when significantly deregulated in deceased donors compared to living donations.

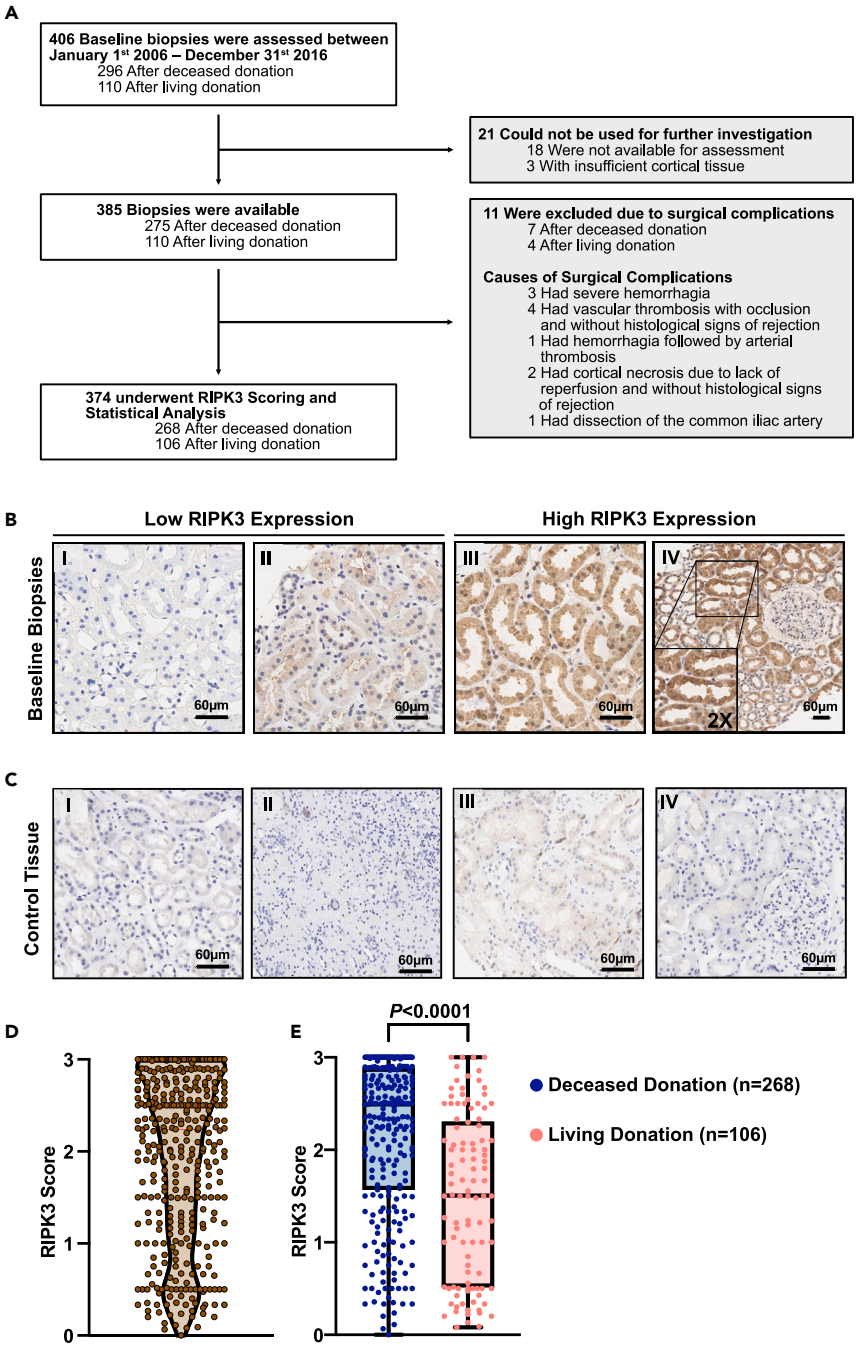

Figure 2. RIPK3 expression levels in baseline biopsies

(A–E) Workflow depicting how baseline biopsies were evaluated for RIPK3 scoring and statistical analysis. From a total of 406 available biopsies, 374 were stained and evaluated within this study. 21 biopsies could not be assessed, and 11 biopsies came from transplants that succumbed to surgical complications, leading to their exclusion (B) Representative images of cortical specimens from baseline biopsies. The exact scores of the illustrated specimens with low and high RIPK3 expression are from left to right as follows: 0; 1.0; 2.34 and 3.0. Scale bars as depicted (C) Representative images of negative controls, specifically, (I) tumor-distant non-inflamed and non-fibrotic renal parenchyma from kidneys after tumor nephrectomy; (II) kidneys from end stage allograft failure with severe interstitial fibrosis and tubular atrophy; (III and IV) kidneys with membranous glomerulonephritis and nephrotic proteinuria. Scale bars as depicted (D) Scatterplot (with median reported in red) depicting the distribution of RIPK3 score across the investigated cohort (E) RIPK3 score is significantly higher in biopsies from deceased donors. Data are presented as scatterplot and in the graph the median is reported. p value from Mann-Whitney test is reported in figure.

Table 1. Demographic and clinical characteristics of the corresponding donors and recipients of the 374 renal allografts[b]

Characteristic	Total	RIPK3 Score ≤2	RIPK3 Score >2	p-value
Specimen	374	163	211	
Donors				
Deceased donation, no. (%)	268 (72)	93 (57)	175 (83)	**<0.001**
If deceased, donor's COD[a], no. (%)				0.553
Cerebrovascular accident	155 (58)	51 (55)	104 (59)	
Trauma	62 (23)	21 (23)	41 (23)	
Others	51 (19)	21 (23)	30 (17)	
Expanded criteria donor, no. (%)	152 (41)	64 (39)	88 (42)	0.633
Combined Pancreas-/Kidney transplantation, no. (%)	10 (3)	4 (3)	6 (3)	0.817
Age [years]	53 ± 15	53 ± 13	52 ± 16	0.472
Female sex, no. (%)	171 (46)	75 (46)	96 (46)	0.921
Donor's last SCr[b] [mg/dL]	0.9 [0.7; 1.1]	0.9 [0.7; 1.0]	0.9 [0.7; 1.2]	0.722
BMI [kg/m^2]	27.0 ± 5.2	27.4 ± 5.6	26.7 ± 4.8	0.16
Known history of hypertension, no. (%)	148 (40)	63 (39)	85 (40)	0.699
Known history of diabetes, no. (%)	34 (9)	10 (6)	24 (11)	**0.027**
Known smoker, no. (%)	110 (29)	47 (29)	63 (30)	0.829
Process				
Cold storage, no. (%)	374 (100)			
Cold ischemia time [h]	8 [2; 13]	6 [2; 10]	10 [5; 14]	**<0.001**
Warm ischemia time [min]	20 [20; 20]	20 [20; 20]	20 [20; 30]	0.094
Recipients				
Age [years]	52 ± 13	52 ± 14	52 ± 13	0.644
Female sex, no. (%)	132 (35)	57 (35)	75 (36)	0.908
Caucasian, no. (%)	367 (98)	159 (98)	208 (99)	0.744
BMI [kg/m^2]	25.2 ± 4.8	25.3 ± 4.5	25.2 ± 4.9	0.765
Repeat transplantation, no. (%)	59 (16)	19 (12)	40 (19)	0.55
No. of HLA-mismatches	4 [3; 5]	4 [3; 5]	4 [3; 5]	0.729
PRA [%], median (range)	0 (0–100)	0 (0–98)	0 (0–100)	0.328
CMV D[a], R-, no (%)	85 (23)	32 (20)	53 (25)	0.276
Additional induction therapy, no. (%)[c]	93 (25)	37 (23)	56 (27)	0.394
Other therapy, no. (%)				
Glucocorticoids	373 (100)	162 (99)[e]	211 100)	0.255
Calcineurin inhibitors [d]	373 (100)	162 (99)[e]	211 (100)	0.255
Tacrolimus	294 (79)	137 (84)	157 (74)	**0.024**
Cause of ESRD, no. (%)				0.106
Glomerulonephritis	110 (29)	58 (36)	52 (25)	
Diabetes	47 (13)	18 (11)	29 (14)	
Hypertension	55 (15)	18 (11)	37 (18)	
Others	134 (36)	59 (36)	75 (36)	
(unknown)	28 (8)	10 (6)	18 (9)	

(*Continued on next page*)

Table 1. *Continued*

Characteristic	Total	RIPK3 Score ≤2	RIPK3 Score >2	p-value
Dialysis vintage [months]	47 [18; 84]	34 [7; 86]	52 [26; 84]	**0.026**
Charlson-comorbidity-score	2 [2; 4]	2 [2; 4]	2 [2; 4]	0.465

n (%) for categorical data, mean ± standard deviation for normally distributed data, median [interquartile range] for non-parametric data. Comparison of groups by χ^2 for categorical data, independent t-test for normally distributed or Mann-Whitney U test for non-parametric data. [a]COD: Cause of death, [b]SCr: Serum-Creatinine, [c]Patients with increased immunologic risk received anti-thymocyte globulins (86 patients (23%)), interleukin-2–receptor blockers (6 patients (2%)), and 1 patient received eculizumab as complement inhibiting induction, in addition to 3-drug immunosuppressive therapy. p values < 0.05 are highlighted in bold.
[d]Calcineurin inhibitors were tacrolimus or cyclosporine.
[e]One recipient received no calcineurin inhibitor or glucocorticoid therapy as a monozygotic twin of the donor.

During observation, four patients were lost to follow-up: one patient after deceased donation after 54 days and three patients after living donation (one after 428 and two after 1096 days of follow-up). Within the first year, 22 patients had a transplant failure and 14 patients died with a functioning allograft. During up to five years after transplantation, 21 additional patients had a transplant failure and 18 additional patients died with a functioning allograft.

Assessment of RIPK3 expression in baseline biopsies and controls

RIPK3 expression varied substantially between the different allograft biopsies. If expressed, RIPK3 was specifically detectable in proximal tubular cells and less prominently in distal tubular cells, which are the cell types mainly affected by IRI. The glomerulus, collecting ducts as well as endothelial cells did not express RIPK3 (Figure 2B). Various negative controls were used to assess the specificity of the RIPK3 stain (Figure 2C). Tubular cells in tumor-distant non-inflamed and non-fibrotic renal parenchyma from kidneys after tumor nephrectomy did not express RIPK3. Similarly, no RIPK3 expression was observed in end-stage transplant failure with severe interstitial fibrosis and tubular atrophy. Lastly, non-specific binding of the RIPK3 antibody to luminal proteins was excluded using kidneys with membranous glomerulonephritis and nephrotic proteinuria. Additionally, staining specificity was confirmed by overexpressing RIPK3 in a human cell line using a human RIPK3-containing vector (Figures S2B and S2C). While RIPK3 expression varied substantially across the biopsies (Figure 2D), it significantly differed between living and deceased donors (Figure 2E).

RIPK3 score and graft outcome

Primary endpoint

Of the 374 allograft biopsies that underwent RIPK3 scoring and statistical analysis, 211 had a RIPK3 score greater than 2 (up to 3), and 163 had a RIPK3 score from 0 to 2. The risk of transplant failure within the first year was significantly higher among allografts with a RIPK3 score greater than 2.0 than among those with a RIPK3 score from 0 to 2.0 (9.2 versus 1.9%; p = 0.003) (Figure 3A). After the first year (two to five-year follow-up observation), there was no significant difference among allografts with a RIPK3 score greater than 2.0 compared to those with a RIPK3 score from 0 to 2.0 (p=0.81). *Of note, we have also performed these analyses by using the median RIPK3 score and obtained similarly significant results (data not shown).* In our cohort, a Cox proportional hazards model revealed several significant univariate predictors of one-year transplant failure. Among other predictors of lower organ quality such as kidneys from deceased donors or from expanded criteria donors, RIPK3 expression as measured by the RIPK3 score proved to be a strong predictor of transplant failure within the first year (hazard ratio: 2.09; 95% CI, 1.13 to 3.87; p=0.019). Expanded criteria donors are donors that are either older than 60 years, or 50–59 years old and meet at least two of the following criteria: cerebrovascular death, history of hypertension, and/or last serum creatinine greater than 1.5 mg/dL.[3] Further, donor age and donor history of hypertension and diabetes were prognostic for one-year transplant failure. Additional factors associated with the recipients – the number of HLA mismatches and the recipient's age – were also associated with the risk of one-year transplant failure (Table 2).

To test whether the RIPK3 score predicts early transplant failure independently of the recipient or donor-associated risk factors, we established multivariate Cox regression models including recipient and donor-associated risk factors from univariate analysis (Table 3). The different calculated models are shown in Table 3. For example, to test whether the RIPK3 score represents lower organ quality independently of the recipient, we established different multivariable Cox regression models including a model with adjustment for the number of HLA mismatches and recipient age. The hazard ratio for the RIPK3 score in this multivariate model was 1.98 (95% CI, 1.06 to 3.71; p=0.033) (Model 3, Table 3). Therefore, RIPK3 expression seems to predict early transplant failure in multivariable analysis independent of donor and recipient characteristics.

Of note, 30% of kidney transplants including baseline biopsies with a RIPK3 score of 0–2 and 36% with a RIPK3 score greater than 2 underwent delayed graft function, defined as a need for dialysis therapy during the first week after transplantation (p = 0.266). To compare the glomerular filtration rate (GFR) between recipients having a baseline biopsy with a RIPK3 score of 0–2 and RIPK3 >2 we provide a supplemental figure (see Figure S3). The GFR during the first year after transplantation was similar in both groups.

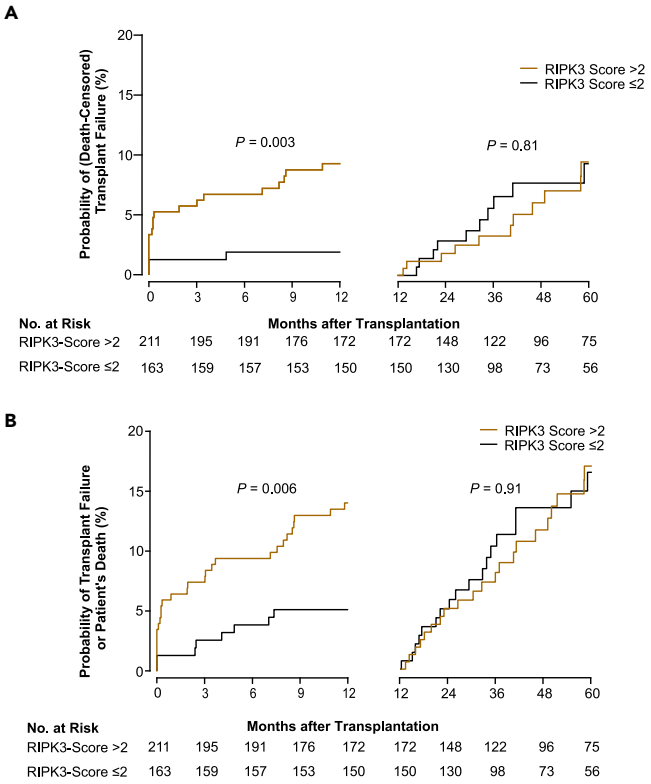

Figure 3. RIPK3 expression predicts kidney transplant failure

(A) Kaplan-Meier estimates of death-censored transplant failure. Shown are estimates of the probabilities of the primary endpoint (i.e., the permanent need for dialysis after transplantation, which consists of both primary non-function (without surgical complications) and follow up end-stage transplant failure requiring the reinstitution of dialysis) comparing renal allograft baseline biopsies with a RIPK3 score of 0–2.0 (≤2) and greater than 2.0 (>2). Estimates are shown for the first year (left) and for the follow up period from year 2–5 (right). Data were censored for death-censored graft survival at the time of death with a functioning graft, at last day of detected kidney function, and either at 12 months (for one-year transplant failure) or at 60 months (for the follow up period 2–5 years). p-Values were calculated using the log rank test.

(B) Kaplan-Meier estimates of non-death-censored transplant failure. Shown are estimates of the probabilities of the secondary endpoint, which was a composite of primary non-function (without surgical complications), follow-up end-stage transplant failure requiring the reinstitution of dialysis, or recipient death with a functioning allograft for renal allograft baseline biopsies, with a RIPK3 score 0 to 2.0 (≤2) and greater than 2.0 (>2). Estimates are shown for first year (left) and for the follow-up period from year 2–5 (right). Data were censored for non-death-censored graft survival at last day of detected kidney function and either at 12 months (for one-year transplant failure) or at 60 months (for the follow-up period 2–5 years. p-values were calculated using the log rank test.

Secondary endpoint

The risk of the non-death-censored transplant failure within the first year was significantly higher among allografts with a RIPK3 score greater than 2 than among those with a RIPK3 score from 0 to 2 (13.5 versus 4.9%, p = 0.006) (Figure 3B). After the first year (2 to 5-year follow-up observation), there was again no relevant difference among allografts with a RIPK3 score greater than 2.0 than among those with a RIPK3 score from 0 to 2.0 (p = 0.91) according to the secondary endpoint.

The Cox proportional hazards model confirmed the RIPK3 score as a significant univariate predictor for the combined endpoint of non-death-censored transplant failure within the first year (hazard ratio: 1.57; 95% CI, 1.03 to 2.39; p = 0.035). Furthermore, deceased donation, expanded criteria donors, and donor age, all representing lower organ quality, were also predictive for non-death-censored transplant failure within the first year, as expected.

Recipient factors that were found to be predictive for non-death-censored transplant failure within the first year were the number of HLA mismatches, the recipient's age, and the recipient's Charlson Comorbidity Score (Table S2). However, in the following multivariable Cox regression model including the number of HLA mismatches, recipient age, and Charlson Comorbidity Score, the RIPK3 score was no longer significantly associated with (non-death-censored) time to transplant failure, including recipient's death with a functioning graft as accepted endpoint (hazard ratio: 1.43; 95% CI, 0.93–2.20; p = 0.10).

Donor and transplantation associations with the RIPK3 score

The median RIPK3 score was significantly higher in kidneys after deceased donation (2.49; Interquartile range {IQR}, 1.57 to 2.89) compared to living donation (1.51; IQR, 0.51 to 2.33; p < 0.001). Furthermore, donor kidneys with a history of diabetes had a significantly greater median

Table 2. Univariate Cox proportional hazards models for one-year death-censored transplant failure with hazard ratios (HR) and 95% confidence intervals (CI) for known risk factors

Risk factors	Univariate HR (95% CI)	p-value
RIPK3 Score	2.09 (1.13–3.87)	**0.019**
Donor associated		
Deceased donation	8.60 (1.16–63.90)	**0.036**
Expanded criteria donor	5.13 (1.89–13.90)	**0.001**
Age [years]	1.07 (1.03–1.12	**<0.001**
Last SCr[a] [mg/dl]	0.91 (0.42–2.09)	0.814
Cerebrovascular COD[b]	2.38 (0.87–6.50)	0.090
Known history of hypertension. 3.35 (1.36–8.20)		**0.008**
Known history of diabetes	3.94 (1.54–10.06)	**0.004**
Sex (female donor)	0.80 (0.34–1.88)	0.614
BMI [kg/m^2]	1.02 (0.96–1.09)	0.531
Transplant associated		
Cold ischemia time [h]	1.05 (0.98–1.12)	0.142
Warm ischemia time [min]	1.00 (0.96–1.05)	0.877
Delayed graft function	1.61 (0.43–5.98)	0.480
Recipient associated		
No. of HLA-mismatches	1.73 (1.22–2.46)	**0.002**
PRA [%]	1.01 (1.00–1.02)	0.112
Recipient age [years]	1.06 (1.02–1.11)	**0.005**
Recipient BMI [kg/m^2]	1.06 (0.98–1.15)	0.138
Repeat transplantation	1.59 (0.84–3.01)	0.155
Dialysis vintage [month]	1.01 (1.00–1.02)	0.345
Charlson comorbidity score	1.08 (0.76–1.54)	0.669

[a]SCr, Serum-Creatinine.
[b]COD, Cause of death.
p values < 0.05 are highlighted in bold.

RIPK3 score than those from donors without diabetes (2.51; IQR, 1.89 to 2.97 versus 2.22; IQR, 1.17 to 2.75; p = 0.034) (Table S3). Additionally, the RIPK3 score correlated significantly with CIT (Spearman's rho, 0.280; p < 0.001) (Table 4).

RIPK3 score and acute tubular injury

There was a relevant correlation between the RIPK3 score and the extent of (acute) tubular injury (Spearman's rho, 0.367; p < 0.001). In line with these results, the frequency of high acute tubular injury was significantly increased for deceased donors (Figure 4A). Next, we further stratified our cohort accordingly to a RIPK3 expression score of 2 and detected the same effect both in the living and in the deceased donor pool (Figures 4B and 4C). Notably, chronic lesions such as glomerulosclerosis, arteriosclerosis, and the extent of interstitial fibrosis and tubular atrophy (IF/TA) in the baseline biopsy according to the common Banff classification did not show any correlation with the RIPK3 Score (Table 4).

Of note, RIPK3 expression is independent of donor and recipient associated risk factors as seen in Table 3 and it correlates with risk factors associated with the transplant process as CIT or Acute tubular injury as seen in (Table 4). Therefore, in further multivariable Cox regression model including RIPK3 expression, CIT and the extent of Acute tubular injury the RIPK3 score was no longer significantly associated with (death-censored) time to one-year transplant failure, (hazard ratio: 1.79; 95% CI, 0.90–3.56; p = 0.095).

DISCUSSION

To the best of our knowledge, this is the first large-scale investigation that provides evidence for a putative role of RIPK3 in human IRI.[26,27] At first, in an unbiased transcriptomic analysis in living versus deceased donor grafts we identified TNF signaling as the most important pathway upregulated in kidney transplantation after deceased donation compared to living donation. Furthermore, we found that RIPK3, the key molecule of necroptosis, was significantly upregulated in these samples. This is tantalizing since many preclinical studies including kidney transplantation could demonstrate that RIPK3 deficiency protected kidneys from IRI-associated damage.[15,16] We thus evaluated RIPK3 protein

Table 3. Multivariate Cox proportional hazards models for one-year death-censored transplant failure with hazard ratios (HR) and 95% confidence intervals (CI) adjusted for donor and recipient associated risk factors

	Model 1	Model 2	Model 3	Model 4	Model 5
Risk factors	HR (95% CI), p-value	HR (95% CI), p-value	HR (95% CI), p-value	HR (95% CI), p-value	HR (95% CI), p-value
RIPK3 Score	2.03 (1.08–3.84), **0.029**	1.97 (1.06–3.69), **0.033**	1.98 (1.06–3.71), **0.033**	2.01 (1.07–3.76), **0.029**	1.96 (1.04–3.69), **0.039**
Donor associated					
Expanded criteria donor	4.64 (1.70–12.67), **0.003**				
Known history of diabetes	2.60 (1.01–6.71), **0.048**				
Donor age		1.06 (1.02–1.10), **0.002**			
Known history of hypertension		1.88 (0.74–4.78), 0.148			
Recipient associated					
Recipient age			1.05 (1.01–1.09), **0.023**		
No. of HLA-mismatches			1.58 (1.11–2.24), **0.012**		
PRA [%]				1.01 (0.99-1-02), 0.30	
Repeat transplantation				1.11 (0.49–2.51), 0.81	
Recipients BMI					1.07 (0.99–1.16), 0.09
Charlson comorbidity score					1.07 (0.74–1.55), 0.71

p values < 0.05 are highlighted in bold.

expression levels, as a proxy for the propensity to undergo necroptosis, in a large cohort of 374 baseline biopsy samples obtained from renal allografts 10 min after the onset of reperfusion.

In our study, higher RIPK3 expression was predictive for one-year transplant failure independent of any factors associated with donor or recipient factors (e.g., HLA-mismatch). This suggests that RIPK3 expression reflects reduced allograft quality, which is affected by ischemia and aggravated by IRI, in turn determining short-term transplant failure.[4] Of note, recent data from a large European cohort showed a trend of decreased improvement in short-term graft survival since 2000.[28] This may reflect the increased use of kidneys from expanded criteria donors to cover the organ demand.[29] High RIPK3 expression shortly after transplantation seemed to play a subordinate role during long-term follow-up as the recipient characteristics and immunological factors (e.g., non-adherence and *de novo* donor-specific antibodies) become more prominent factors.[30,31]

RIPK3 expression was further prognostic for the combined endpoints of transplant failure and patient's death with functioning allograft within the first year, but not independent of the recipient's health condition. These results are plausible because death frequently depends on the comorbidities of the recipient. Hence, to investigate organ quality affected by IRI, death-censored transplant failure is the most representative primary endpoint because it is less dependent on the recipient.

A tendency to higher RIPK3 expression in organs with lower quality was underlined by higher RIPK3 levels in kidneys from deceased or diabetic donors.[19] We could further show the impact of IRI on RIPK3 expression. The RIPK3 score correlated with CIT and the extent of acute tubular injury, the histological hallmark of IRI. This aligns with the growing body of evidence, that RIPK3-dependent necroptosis plays a central pathophysiological role in IRI and acute tubular injury.[9] Recently, in a murine transplant model, it has been shown that donor kidneys subjected to cold ischemia followed by transplantation showed higher expression of RIPK3 than donor kidneys subjected to transplantation without cold ischemia.[32] Our human data are in line with these preclinical findings.

Limitations of the study

Our study has several limitations and some points for critical discussion. First, we used a single-center cohort without multicentric validation. Nevertheless, this represents one of the largest studies correlating protein expression with clinical outcomes. Second, we chose death-censored transplant failure with a permanent need for dialysis as the primary endpoint. This is challenging for transplant studies with an expected low incidence of the primary endpoint in a single-center cohort. However, we explicitly decided not to use an alternative combined endpoint, including doubling of serum creatinine,[33] since this endpoint does not adequately reflect organ quality following severe IRI within the first year. Also, it is conceivable, that possible long-term effects of initially high RIPK3 expression were not noted due to the low number of

Table 4. Association of the RIPK3 Score with possible allograft and storage characteristics concerning organ quality

Factors	RIPK3 Score rho[b]	p value
Donor		
Age	−0.048	0.352
Donor's Last SCr[a] [mg/dL]	0.071	0.173
Ischemia		
Cold ischemia time [h]	**0.280**	**<0.001**
Warm ischemia time [min]	0.100	0.053
Baseline biopsy		
Acute tubular injury	**0.367**	**<0.001**
IF/TA [%]	0.007	0.891
Arteriolosclerosis[c]	−0.011	0.848
Glomerulosclerosis [%]	−0.038	0.491

[a]Analysis was done using Spearman's rho.
[b]SCr, Serum-Creatinine.
[c]Arteriolosclerosis was assessed according to BANFF classification.
p values < 0.05 are highlighted in bold.

events due to the primary endpoint and the heterogeneous follow-up time based on the different inclusion time points (2006–2016) with a median of 4.6 years. Third, in our cohort, the CIT was not predictive of transplant failure in the univariate Cox model. This could be due to the relatively short CIT, with a median of 8 h (mean CIT, 8.8 h; range from 1 to 28 h), which is due to the relevant percentage (28%) of living donors. A recent observational multicentric study with 3839 patients showing an influence of CIT on graft survival had a mean CIT of 20.6 h (ranging from 6 to 58.6 h).[34] However, we could demonstrate a direct correlation between RIPK3 expression and CIT by a Spearman's correlation analysis, and an indirect correlation by showing higher RIPK3 levels in kidneys from deceased donors with a significantly longer CIT than kidneys from living donors. Thus, we speculate that RIPK3 expression could be an even stronger predictor in cohorts of donor kidneys that are exposed to longer CIT.

Importantly, when this study was initiated, the field was still confronted with a scarcity of commercially available antibodies for staining RIPK3. Therefore, this study of IHC analysis of human baseline biopsies is restricted to the use of a single RIPK3 antibody. While we have asserted the cell type specificity, overexpression, and subsequent knockdown of RIPK3 detected by the antibody used (Figures S2A–S2C), it is clear that there is an urgent need for the development of antibodies showing less unspecific signals in human cells. Therefore, in light of their translational value, we believe that future studies will be critical to validate these findings using a broader array of improved RIPK3-specific antibodies. Already today a broad effort is underway to achieve this aim, building upon which we and others will continue to test the clinical validity of the findings presented herein.

Finally, we did not directly show necroptosis activation in samples with high RIPK3 expression, which is difficult in primary formalin-fixed human samples. However, our RNA-seq data hinted at regulated cell death in human renal IRI. Further, the high RIPK3 expression demonstrates the high prevalence of the protein. Based on preclinical findings,[17] we infer that cells with high RIPK3 expression show a greater propensity to undergo programmed cell death at any time than those with low expression.

Concluding remarks

In conclusion, our data suggest that RIPK3 might play a critical role in tissue injury during human transplantation. Future interventional studies aiming to prevent RIPK3 expression in kidneys with severe IRI are worth investigating, for example, by *ex vivo* perfusion with necroptosis-inhibiting agents, some of which have already been approved for use in humans.

STAR★METHODS

Detailed methods are provided in the online version of this paper and include the following:

- KEY RESOURCES TABLE
- RESOURCE AVAILABILITY
  - Lead contact
  - Materials availability
  - Data and code availability
- EXPERIMENTAL MODEL AND STUDY PARTICIPANT DETAILS
  - Description of the cohort and baseline biopsies

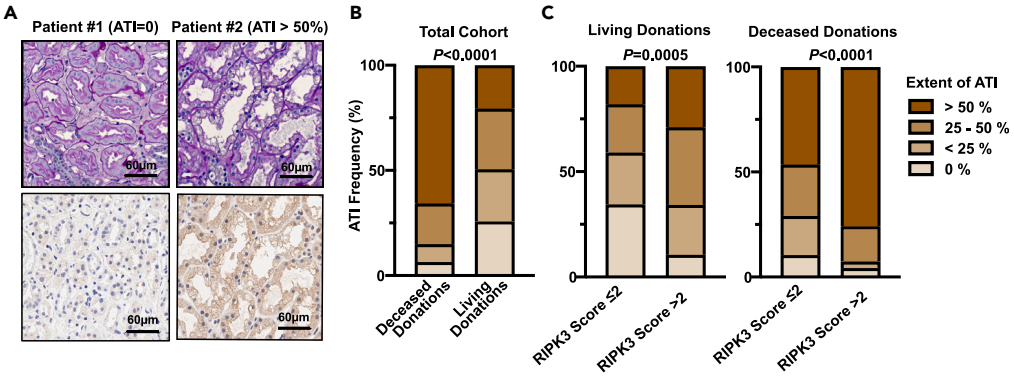

Figure 4. RIPK3 expression and its association with acute tubular injury

(A) Representative images of PAS reaction of cortical specimen with corresponding RIPK3 staining. Scale bar as depicted.

(B and C) Frequency distribution of acute tubular injury (ATI) in the whole cohort. p-value from chi-square test is reported in figure (C) Frequency distribution of ATI in living and deceased donation cohorts, stratified above and below the RIPK3 score median. p value from chi-square test is reported in figure.

SUPPLEMENTAL INFORMATION

Supplemental information can be found online at https://doi.org/10.1016/j.isci.2023.107879.

ACKNOWLEDGMENTS

We thank Sandra Haderer, Alina Schmidt, and Olga Seelbach (CEP, TUM) for excellent technical assistance and the tissue bank (MTBIO) of the TUM and MRI for tissue handling. This work was supported by research grants from the DFG FOR2036 JO 1179/1-1, SFB 1335, SFB 1350 (C2), an MD stipend for A.W. from DZIF 80245MDADW, a grant from Else Kroner-Fresenius Foundation P27/10//A33/10 to C.S., DFG 405101514 to M.Y.

AUTHOR CONTRIBUTIONS

S.K., A.W., and C.S. designed the concept of the study and S.K. was the PI of the study. S.K. and C.S. were responsible for clinical data management. A.W. was responsible for the histological assessment of RIPK3 expression. S.K. performed the statistical analysis. A.W. performed RIPK3 scoring. M.B-H. analyzed the biopsies including the extent of acute tubular injury. K.S. and J.S-H. supervised the immunohistochemical staining and reviewed RIPK3 scoring. J.S. performed the cell-type specific staining. S.D., R.Ö., T.E., and R.R. performed the transcriptome analysis. T.S. and C.B. performed antibody validation. S.K., F.H., C.T., and Q.B. collected clinical follow-up data. S.K. and C.S. analyzed the clinical follow-up data. G.L., R.G., B.H., and M.C.B. supported the statistical analysis of the follow-up data. E.M., V.A., and S.T. performed the surgical biopsies used in this study. J.H.B., M.Y., P.M., L.R., U.H., W.W., S.V.V., M.S., R-U.M., D.L.S., O.V., and K.A., resources, and critical discussions. D.G. and A.L., guidance for the design of the study. S.K. and A.W. wrote the manuscript, and C.S. edited and revised the manuscript. All authors discussed the results and contributed to the manuscript.

DECLARATION OF INTERESTS

No author declares a conflict of interest.

INCLUSION AND DIVERSITY

We support inclusive, diverse, and equitable conduct of research.

Received: July 2, 2022
Revised: October 5, 2022
Accepted: September 7, 2023
Published: September 17, 2023

REFERENCES

1. Hart, A., Lentine, K.L., Smith, J.M., Miller, J.M., Skeans, M.A., Prentice, M., Robinson, A., Foutz, J., Booker, S.E., Israni, A.K., et al. (2021). OPTN/SRTR 2019 Annual Data Report: Kidney. Am. J. Transplant. *21* (*Suppl 2*), 21–137.
2. Tullius, S.G., and Rabb, H. (2018). Improving the Supply and Quality of Deceased-Donor Organs for Transplantation. N. Engl. J. Med. *378*, 1920–1929.
3. Querard, A.H., Le Borgne, F., Dion, A., Giral, M., Mourad, G., Garrigue, V., Rostaing, L., Kamar, N., Loupy, A., Legendre, C., et al. (2018). Propensity score-based comparison of the graft failure risk between kidney transplant recipients of standard and expanded criteria donor grafts: Toward increasing the pool of marginal donors. Am. J. Transplant. *18*, 1151–1157.
4. Foroutan, F., Friesen, E.L., Clark, K.E., Motaghi, S., Zyla, R., Lee, Y., Kamran, R., Ali, E., De Snoo, M., Orchanian-Cheff, A., et al. (2019). Risk Factors for 1-Year Graft Loss After Kidney Transplantation: Systematic Review and Meta-Analysis. Clin. J. Am. Soc. Nephrol. *14*, 1642–1650.
5. Gill, J., Dong, J., Rose, C., and Gill, J.S. (2016). The risk of allograft failure and the survival benefit of kidney transplantation are complicated by delayed graft function. Kidney Int. *89*, 1331–1336.
6. Hall, I.E., Reese, P.P., Doshi, M.D., Weng, F.L., Schröppel, B., Asch, W.S., Ficek, J., Thiessen-Philbrook, H., and Parikh, C.R. (2017). Delayed Graft Function Phenotypes and 12-Month Kidney Transplant Outcomes. Transplantation *101*, 1913–1923.
7. Siedlecki, A., Irish, W., and Brennan, D.C. (2011). Delayed graft function in the kidney transplant. Am. J. Transplant. *11*, 2279–2296.
8. Wekerle, T., Segev, D., Lechler, R., and Oberbauer, R. (2017). Strategies for long-term preservation of kidney graft function. Lancet *389*, 2152–2162.
9. Belavgeni, A., Meyer, C., Stumpf, J., Hugo, C., and Linkermann, A. (2020). Ferroptosis and Necroptosis in the Kidney. Cell Chem. Biol. *27*, 448–462.
10. Linkermann, A., and Green, D.R. (2014). Necroptosis. N. Engl. J. Med. *370*, 455–465.
11. Linkermann, A., Stockwell, B.R., Krautwald, S., and Anders, H.-J. (2014). Regulated cell death and inflammation: an auto-amplification loop causes organ failure. Nat. Rev. Immunol. *14*, 759–767.
12. Pasparakis, M., and Vandenabeele, P. (2015). Necroptosis and its role in inflammation. Nature *517*, 311–320.
13. Sarhan, M., Land, W.G., Tonnus, W., Hugo, C.P., and Linkermann, A. (2018). Origin and Consequences of Necroinflammation. Physiol. Rev. *98*, 727–780.
14. Zhang, T., Zhang, Y., Cui, M., Jin, L., Wang, Y., Lv, F., Liu, Y., Zheng, W., Shang, H., Zhang, J., et al. (2016). CaMKII is a RIP3 substrate mediating ischemia- and oxidative stress-induced myocardial necroptosis. Nat. Med. *22*, 175–182.
15. Linkermann, A., Bräsen, J.H., Darding, M., Jin, M.K., Sanz, A.B., Heller, J.O., De Zen, F., Weinlich, R., Ortiz, A., Walczak, H., et al. (2013). Two independent pathways of regulated necrosis mediate ischemia-reperfusion injury. Proc. Natl. Acad. Sci. USA *110*, 12024–12029.
16. Lau, A., Wang, S., Jiang, J., Haig, A., Pavlosky, A., Linkermann, A., Zhang, Z.-X., and Jevnikar, A.M. (2013). RIPK3-mediated necroptosis promotes donor kidney inflammatory injury and reduces allograft survival. Am. J. Transplant. *13*, 2805–2818.
17. Linkermann, A. (2016). Nonapoptotic cell death in acute kidney injury and transplantation. Kidney Int. *89*, 46–57.
18. Linkermann, A., Chen, G., Dong, G., Kunzendorf, U., Krautwald, S., and Dong, Z. (2014). Regulated cell death in AKI. J. Am. Soc. Nephrol. *25*, 2689–2701.
19. Grams, M.E., Sang, Y., Levey, A.S., Matsushita, K., Ballew, S., Chang, A.R., Chow, E.K.H., Kasiske, B.L., Kovesdy, C.P., Nadkarni, G.N., et al. (2016). Kidney-Failure Risk Projection for the Living Kidney-Donor Candidate. N. Engl. J. Med. *374*, 411–421.
20. van Loo, G., Bertrand, M.J.M., Death by TNF: a road to inflammation. Nat. Rev. Immunol. *23*, 289–303.
21. Bossaller, L., Chiang, P.-I., Schmidt-Lauber, C., Ganesan, S., Kaiser, W.J., Rathinam, V.A.K., Mocarski, E.S., Subramanian, D., Green, D.R., Silverman, N., et al. (2012). Cutting edge: FAS (CD95) mediates noncanonical IL-1β and IL-18 maturation via caspase-8 in an RIP3-independent manner. J. Immunol. *189*, 5508–5512.
22. Hubbard, N.W., Ames, J.M., Maurano, M., Chu, L.H., Somfleth, K.Y., Gokhale, N.S., Werner, M., Snyder, J.M., Lichauco, K., Savan, R., et al. (2022). ADAR1 mutation causes ZBP1-dependent immunopathology. Nature *607*, 769–775.
23. Najjar, M., Saleh, D., Zelic, M., Nogusa, S., Shah, S., Tai, A., Finger, J.N., Polykratis, A., Gough, P.J., Bertin, J., et al. (2016). RIPK1 and RIPK3 Kinases Promote Cell-Death-Independent Inflammation by Toll-like Receptor 4. Immunity *45*, 46–59.
24. Micheau, O., and Tschopp, J. (2003). Induction of TNF receptor I-mediated apoptosis via two sequential signaling complexes. Cell *114*, 181–190.
25. Shikama, Y., Yamada, M., and Miyashita, T. (2003). Caspase-8 and caspase-10 activate NF-kappaB through RIP, NIK and IKKalpha kinases. Eur. J. Immunol. *33*, 1998–2006.
26. Pefanis, A., Ierino, F.L., Murphy, J.M., and Cowan, P.J. (2019). Regulated necrosis in kidney ischemia-reperfusion injury. Kidney Int. *96*, 291–301. https://doi.org/10.1016/j.kint.2019.02.009.
27. Moeckel, G.W. (2018). Pathologic Perspectives on Acute Tubular Injury Assessment in the Kidney Biopsy. Semin. Nephrol. *38*, 21–30.
28. Coemans, M., Süsal, C., Döhler, B., Anglicheau, D., Giral, M., Bestard, O., Legendre, C., Emonds, M.P., Kuypers, D., Molenberghs, G., et al. (2018). Analyses of the short- and long-term graft survival after kidney transplantation in Europe between 1986 and 2015. Kidney Int. *94*, 964–973.
29. Jardine, A.G., Hartmann, A., and Holdaas, H. (2018). Long-term renal allograft survival: a quiet revolution. Kidney Int. *94*, 853–855.
30. Sellarés, J., de Freitas, D.G., Mengel, M., Reeve, J., Einecke, G., Sis, B., Hidalgo, L.G., Famulski, K., Matas, A., and Halloran, P.F. (2012). Understanding the causes of kidney transplant failure: the dominant role of antibody-mediated rejection and nonadherence. Am. J. Transplant. *12*, 388–399.
31. Wiebe, C., Gibson, I.W., Blydt-Hansen, T.D., Karpinski, M., Ho, J., Storsley, L.J., Goldberg, A., Birk, P.E., Rush, D.N., and Nickerson, P.W. (2012). Evolution and clinical pathologic correlations of de novo donor-specific HLA antibody post kidney transplant. Am. J. Transplant. *12*, 1157–1167.
32. Jain, S., Plenter, R., Nydam, T., and Jani, A. (2020). Injury Pathways That Lead to AKI in a Mouse Kidney Transplant Model. Transplantation *104*, 1832–1841. https://doi.org/10.1097/TP.0000000000003127.
33. Coresh, J., Turin, T.C., Matsushita, K., Sang, Y., Ballew, S.H., Appel, L.J., Arima, H., Chadban, S.J., Cirillo, M., Djurdjev, O., et al. (2014). Decline in estimated glomerular filtration rate and subsequent risk of end-stage renal disease and mortality. JAMA *311*, 2518–2531.
34. Debout, A., Foucher, Y., Trébern-Launay, K., Legendre, C., Kreis, H., Mourad, G., Garrigue, V., Morelon, E., Buron, F., Rostaing, L., et al. (2015). Each additional hour of cold ischemia time significantly increases the risk of graft failure and mortality following renal transplantation. Kidney Int. *87*, 343–349.
35. Transplantation, Ebpg Expert Group on Renal (2002). European best practice guidelines for renal transplantation. Section IV: Long-term management of the transplant recipient. IV.13 Analysis of patient and graft survival. Nephrol. Dial. Transplant. *17* (*Suppl 4*), 60–67.
36. Schemper, M., and Smith, T.L. (1996). A note on quantifying follow-up in studies of failure time. Contr. Clin. Trials *17*, 343–346.

STAR★METHODS

KEY RESOURCES TABLE

REAGENT or RESOURCE	SOURCE	IDENTIFIER
Antibodies		
Rabbit polyclonal anti-RIPK3	ProSci	2283; RRID: AB_203256
Mouse monoclonal anti-CK7 (OV-TL 12/30)	Agilent	M7018
Mouse monoclonal anti-CD10	Thermo Fisher Scientific	MA5-14050
Mouse monoclonal anti-EMA (E29)	Sigma-Aldrich	247M-9
Alexa Fluor® 555-conjugated goat anti-rabbit IgG	Lifetechnologies (Thermo Fisher Scientific)	A-21428
Alexa Fluor® 488-conjugated donkey anti-mouse IgG	Invitrogen	10544773
Alexa Fluor® 647-conjugated goat anti-rabbit	Thermo Fisher Scientific	A-21245
Mouse monoclonal anti-GAPDH	Santa Cruz	Sc-47724
Rabbit monoclonal anti-HA	Cell Signaling	3724S
Rabbit monoclonal anti-HSP90	Cell Signaling	4877S
Bacterial and virus strains		
NEB 5-alpha competent E. coli	New England Biolabs	C2987H
Chemicals, peptides, and recombinant proteins		
Maxima Reverse Transcriptase	Thermo Fisher Scientific	EP0742
BES buffered saline	Sigma-Aldrich	14280
Lipofectamine™ RNAiMAX Transfection Reagent	Thermo Fisher Scientific	13778075
siRNA Non-targeting Control SMART Pool	Dharmacon	D-001810-10-05
siRNA RIPK3 ON-TARGETplus SMART Pool	Dharmacon	SO-3127756G
Critical commercial assays		
LEV RNA FFPE Purification Kit	Promega	AS1260
TURBO DNA-free™ Kit	Thermo Fisher Scientific	AM1907
Nextera XT kit	Illumina	FC-131-1002
peqGOLD Plasmid Miniprep Kit	Peqlab	13-6943-02
NucleoBond Xtra Midi	MACHEREY-NAGEL	740420.50
DC™ Protein Assay Kit I	Bio-Rad	5000111
Experimental models: Cell lines		
HEK293T human embryonic kidney cells	ATCC	CRL-3216
Recombinant DNA		
pcDNA3-HA-RIPK3 plasmid	Jaewhan Song	Addgene plasmid # 78804; http://n2t.net/addgene:78804; RRID:Addgene_78804
Software and algorithms		
Aperio Imagescope software Version 12.3	Leica BIOSYSTEMS	https://www.leicabiosystems.com/de-de/digitalpathologie/verwaltung/aperio-imagescope/
IBM SPSS Statistics Version 25	IBM Corp	https://www.ibm.com/support/pages/downloading-ibm-spss-statistics-25

(*Continued on next page*)

Continued

REAGENT or RESOURCE	SOURCE	IDENTIFIER
R Version 3.4.4		https://cran.r-project.org/bin/windows/base/old/
GraphPad Prism version 7.0		https://www.graphpad.com/support/prism-7-updates/
clustVis software	Metsalu, Tauno and Vilo, Jaa	https://biit.cs.ut.ee/clustvis/
GSEAv4.0.3	Broad Institute UCSan Diego	https://www.gsea-msigdb.org/gsea/index.jsp
Cytoscape v3.8.233	National Institute of General Medical Sciences (NIGMS)	Cytoscape v3.8.233
METASCAPE34	Zhou et al.	https://metascape.org/gp/index.html#/main/step1
Dropseq tools v1.12	GitHub Broad Institute	https://github.com/broadinstitute/Drop-seq
Other		
Automated immunostainer Leica Bond RXm	Leica BIOSYSTEMS	
Automated slide scanner AT-2	Leica BIOSYSTEMS	
Automated nucleic acid extraction system Promega Maxwell RSC16	Promega	
Invitrogen™ Qubit™Fluorometer	Thermo Fisher Scientific	15387293
QuBit RNA high-sensitivity kit	Thermo Fisher Scientific	10320093
Metafer Slide-Scanning System	MetaSystems Hard- & Software GmbH, Altlussheim, Germany	
Leica® TCS SP8 confocal microscopy	Leica BIOSYSTEMS	
NextSeq 500	Illumina	

RESOURCE AVAILABILITY

Lead contact

Further information and requests for resources and reagents should be directed to and will be fulfilled by the lead contact, Stephan Kemmner, MD (stephan.kemmner@tum.de).

Materials availability

No new reagents were created during the course of this study.

Data and code availability

This paper does not report original code. All data from patients are available upon reasonable request from the lead contact.

EXPERIMENTAL MODEL AND STUDY PARTICIPANT DETAILS

Description of the cohort and baseline biopsies

All patients included in this retrospective analysis underwent kidney transplantation (or combined pancreas and kidney transplantation) between January 1st, 2006, and December 31st, 2016, at Klinikum rechts der Isar, Munich, Germany, and had a baseline kidney biopsy during surgery. These baseline biopsies were routinely taken intraoperatively 10 min after reperfusion of the organ by core needle (18G) biopsy. This is part of the standard of care protocol to allow initial assessment of graft quality. All biopsies were fixed in 4% neutral buffered formaldehyde and subsequently paraffin-embedded (FFPE) and retrospectively assessed for chronic and acute histological lesions. For detailed routine histological assessment see the supplemental methods. Biopsies before 2006 were not included to ensure the quality of immunohistochemical staining.

METHOD DETAILS

Transcriptomic analysis

For the transcriptomic analysis, RNA was isolated from FFPE biopsy specimens for subsequent RNA sequencing. The primary bioinformatic analysis included Gene set enrichment and weighted gene co-expression network and pathway analyses. Comprehensive methods are described in the supplement. The included cohort consisted of 17 transplant biopsies from living and deceased donors. The transcriptomic analysis of the selected cohort was approved by the local ethics committee of the Technical University of Munich, Germany (No. 594/21 S-KK).

RIPK3 immunohistochemistry and semiquantitative scoring

Immunohistochemistry was performed on an automated immunostainer (Leica Bond RXm) using an antibody against RIPK3 (2283, ProSci). The validation of the RIPK3 antibody is described in the supplement. The stained slides were scanned using an automated slide scanner (AT-2, Leica Biosystems). Subsequently, representative images for scoring were collected using Aperio Imagescope software (version 12.3, Leica Biosystems). To ascertain RIPK3 expression in the stained kidney biopsies we established a semi-quantitative score that assesses the overall (cortical) RIPK3 expression. In brief, RIPK3 expression in cortical tubules from each biopsy was first evaluated by assigning a score for different levels of RIPK3 staining, ranging from 0 (no staining) to 3 (strong staining). Secondly, the sum of all scored tubules was divided by the total number of all examined tubules to assess the overall cortical RIPK3 expression, referred to as the RIPK3 score. The RIPK3 score was ascertained in a blinded fashion to exclude observer bias. In detail, the staff responsible for RIPK3 scoring was not involved in clinical data acquisition and evaluation and was unaware of any clinical information or further clinical course of renal allografts and recipients.

QUANTIFICATION AND STATISTICAL ANALYSIS

Outcome

The primary endpoint was death-censored transplant failure (including primary non-function), comprising the permanent need for dialysis after transplantation. In the event of death with a functioning graft, the follow-up period was censored at the date of death.[35] Graft failure was assessed within one year and five years after transplantation. Patients were censored at one year, five years or at the last day of detected kidney function in follow-up examination within five years.

Primary non-function was defined as an initial non-working allograft with cessation of intermittent dialysis after transplantation, without perioperative complications and with proven organ perfusion confirmed by ultrasound examination.

The secondary endpoint was non-death-censored transplant failure. Thereby, death with a functioning allograft was treated as graft failure. Furthermore, we hypothesized that RIPK3 expression is associated with factors representing limited organ quality and extended transport, such as donor risk factors (age, deceased donation, expanded criteria donor), cold ischemia time (CIT), and histological findings in the baseline biopsy represented histologically as the extent of (acute) tubular injury.

Statistical analysis

The reverse Kaplan-Meier estimator for potential follow-up was used to quantify the length of follow-up time.[36] Kaplan-Meier analysis, univariate and multivariate Cox proportional-hazards analysis and log rank tests were used to examine the association between the RIPK3 score and the primary endpoint. Based on the histological appearance and clinical practicability of the RIPK3 score, we divided patients into two groups with a RIPK3 score of 0–2.0 and higher than 2.0. This division was close to the median RIPK3 score (2.2). At first, Kaplan-Meier analysis was confined to the first year to investigate early transplant failure. Further, all patients with a functioning allograft after the first year were included in an additional 2-5-year Kaplan-Meier analysis to investigate extended follow-up allograft failure.

Univariate and multivariable Cox proportional-hazards analyses were confined to the first year representing early transplant failure due to organ quality. For the estimation of hazard ratios, Cox proportional hazards models were fitted to the data. After detecting univariate associations of donor and recipient risk factors with death-censored and non-death-censored transplant failure, we fitted multivariable models including recipient and donor-associated risk factors from univariate analysis for the primary endpoint. All tests were performed two-sided using a significance level of $\alpha = 0.05$. We used IBM SPSS Statistics, version 25 (IBM Corp., NY, USA) and R version 3.4.4 (R development core team, Vienna, Austria) for all statistical analyses and GraphPad Prism, version 7.0 (Graph-Pad Software), for data visualization.